Proteomic identification of down-regulation of oncoprotein DJ-1 and proteasome activator subunit 1 in hepatitis B virus-infected well-differentiated hepatocellular carcinoma

DAOHAI ZHANG[1,2*], SENG GEE LIM[3] and EVELYN S.C. KOAY[1,2*]

[1]Department of Laboratory Medicine, National University Hospital; Departments of [2]Pathology, and [3]Medicine, Yong Loo Lin School of Medicine, National University of Singapore, Singapore 119074

Abstract. Hepatocellular carcinoma (HCC) is a common malignant tumour. Development of HCC is a multi-step process from well-differentiated (G1), moderately differentiated (G2) to poorly differentiated (G3) phenotype. The early molecular modulators causing the onset of hepatocarcinogenesis are not fully understood. In the present study, we conducted comparative proteomics to analyze the differential proteome of G1 tumour and adjacent non-tumour tissues, with aims to identify the molecules as early tumour markers and to understand the early molecular events involved in initiation of tumorigenesis in hepatitis B virus (HBV)-infected G1 tumour. Differentially expressed proteins were identified by MALDI-TOF/TOF tandem mass spectrometry and NCBInr database interrogation. A total of 15 differentially expressed proteins with diverse biological functions were identified. Among these, 4 proteins were down-regulated, whereas the other 11 proteins were up-regulated in the G1 tumours. Two proteins, Proteasome activator subunit 1 (PA28α) and DJ-1, were firstly found to be down-regulated in HBV-infected G1 tumours. Down-regulations of these two proteins were further validated by Western blotting and immunohistochemistry in a panel of clinical specimens. These findings elucidate, at least in part, the molecular events underlying the mechanism and the potential roles of DJ-1 and PA28α in the onset of hepatocarcinogenesis.

Introduction

Hepatocellular carcinoma (HCC) develops from a chronic inflammatory liver disease caused by hepatitis B or C virus, alcohol abuse, exposure to carcinogen such as aflatoxin B1, and genetic alteration, etc. (1). The high incidence of death of patients with HCC is mainly due to the lack of a valuable prognostic indicator and effective treatment. There are a few biomarkers for clinical diagnosis in HCC: α-fetoprotein (AFP), des-γ-carboxy prothrombin plasma abnormal prothrombin, the L3 fraction (AFP-L3), isozyme of alkaline phosphatase (variant ALP), and isozyme of γ-glutamyl transpeptidase (novel γ-GTP) (2). However, considering the sensitivity, specificity and operability, only AFP is a useful marker in the diagnosis of HCC, especially HBV-associated HCC. Nevertheless, the AFP level is normal in up to 30% of patients with liver cancer, and other factors including early childhood liver damage from hepatitis, or tumours of the testis can also raise the AFP level. Therefore, as an HCC tumour marker, the AFP test has minimal clinical significance and must be interpreted together with a proper imaging diagnosis of the liver.

Recently, the proteomics approach has been widely used in discovering tumour-associated biomarker/drug targets and in deciphering the molecular mechanism underlying the tumorigenesis. In HCC, many potential markers have been identified from clinical tissue specimens using different proteomic approaches, including laser capture microdissection (LCM), isotope-coded affinity Tag (ICAT), two-dimensional gel electrophoresis (2-DE), two-dimensional difference gel electrophoresis (2-D-DIGE) and mass spectrometry (3-9). Such analyses have revealed the complicated molecular repertoire of markers which are involved in a variety of biological functions including signal transduction, metabolism and apoptosis. Unfortunately, only a few of the protein markers have been validated in clinical specimens due to the lack of available antibodies or due to the large-scale labour-intensive work involved in the validation process. Among them, alteration of aldehyde dehydrogenase isozyme closely correlated to HCC (10), and human aldose reductase-like protein-1 was suggested to be a strong candidate as an

---

immunohistochemical diagnostic marker (6). Further, the Hsp27 expression correlated with the level of AFP but not with tumour stage (5), although it was considered to be a potential serum biomarker in patients with HCC (11). Other potential markers include α-enolase whose level correlated to HCV-infected HCC tumour progression (12) and protein C3a whose expression was elevated in patients with HCV-related HCC (13). Nevertheless, clinical validation and application of the tumour-marker candidates are an urgent requirement in cancer translational interface.

HCC is developed from a multi-step process based on histologic changes: tumour cells are initially well differentiated (grade 1, G1), and then progress to moderately differentiated (grade II, G2) and poorly differentiated (grade III, G3) types with high proliferation rates. Evidence has shown that the proteome profiles of HCC tumours are grade-dependent. In HCC, cytokeratin 19 (CK19) was highly expressed in the late stage of tumours (G3) and strongly related to metastatic behaviour (14). α-enolase was strongly expressed in G3 tumours compared with G1 and G2 tumours (12), and glutamine synthetase was highly expressed in HCV-infected G1 tumours (15). Recently, protein Hcc-2 was found to be up-regulated in G3 tumours but unchanged in G1 tumours (16). In addition, proteome profiles of HCC are also virus-dependent. Previous study demonstrated that HCC proteome and gene expression profiling vary between HBV- and HCV-infected HCC tumours (8,17). Kim et al found that Hsp27 was down-regulated in HBV-related HCC, but up-regulated in HCV-related HCC, whereas ECH1 was highly expressed in HCV-infected HCC, but decreased in HBV-infected HCC tumours with no clarification of tumour grade (8). As such, the HCC specimens for proteomics study should be carefully selected when addressing the relevance of molecular alterations with specific aetiology and/or histopathological features.

In the present study, we analyzed the differential proteome profiles between HBV-infected G1 tumour and adjacent non-tumour tissues in order to identify the potential molecules as early tumour markers and to understand the early molecular events involved in initiation of tumorigenesis. We have identified 15 dysregulated proteins with varieties of biological functions by MALDI-TOF/TOF tandem mass spectrometry and NCBInr database interrogation. Two proteins including oncoprotein DJ-1 and proteasome activator subunit 1 (PA28α) were, for the first time, found to be down-regulated in the HBV-infected G1 tumour. Their roles in hepatocarcinogenesis and potentials as early biomarkers for cancer diagnosis are discussed.

Materials and methods

Tissue specimens. Six pairs of human HBV-infected (G1) HCC frozen tumour tissues and the adjacent non-tumour tissues were provided by Professor SG Lim, Department of Medicine, National University Hospital. The HCC tissue collections were obtained under informed consent and were approved by the ethics committee of the hospital. These tumour specimens were diagnosed as well differentiated (G1) by pathological examination, according to the method described by Desmet *et al* (18). These tumour/non-tumour tissues were used for proteome analysis.

Protein extraction and protein separation by 2-dimensional electrophoresis (2-DE). For each sample, the frozen liver tissue was transferred to a pre-cooled mortar, ground to powder in liquid nitrogen, and solubilized in Tissue Protein Extraction Reagent® (Pierce, Rockford, IL, USA) according to the manufacturer's protocol. Samples were cleaned up using a PlusOne 2-D Clean-up kit (GE Healthcare, San Francisco, CA, USA) and re-dissolved in sample buffer (7 M urea, 2 M thiourea, 4% CHAPS, 1% Mega-10, 0.5% Triton x-100, 50 mM dithiothreitol, 1% IPG buffer (pH 4-7) and 2 mM tributyl phosphine). Protein concentrations were determined using the PlusOne 2-D quantitation kit (GE Healthcare).

2-DE and image analysis were performed as described previously (19). Briefly, equal amounts (120 μg) of proteins from tumour and matched non-tumour tissues were separately mixed with 350 μl of rehydration solution containing 7 M urea, 2 M thiourea, 4% CHAPS, 0.5% IPG buffer (pH 4-7), and rehydrated for 12 h at 20 V using the Immobiline IPG DryStrips (180 mm, pH 4-7) (GE Healthcare). Proteins were isoelectrically focused at 500 V for 1 h, 2000 V for 1 h, 4000 V for 2 h and 8000 V for 6 h on an Ettan IPGphor electrophoresis system (GE Healthcare). After equilibration for 2x15 min in equilibration buffer, IPG strips were applied for SDS-PAGE (12%) using a PROTEAN® II xi Cell system (Bio-Rad, Hercules, CA, USA). The separated proteins were visualized by silver staining (19).

Image acquisition and analysis. Silver-stained gels were scanned using the Personal SI densitometer (Molecular Dynamics, Sunnyvale, CA, USA). Spot detection, matching and expression levels of proteins on 2-DE gels were quantitatively analyzed, based on the spot intensities, using the ImageMaster 2D Elite software (GE Healthcare). Differences in expression levels between paired samples were analyzed by Student's t-test. Protein spots showing at least 2-fold changes (p<0.05) in intensity were picked for trypsin digestion and MALDI-TOF/TOF MS/MS analysis.

Trypsin in-gel digestion and mass spectrometry. The protein spots were manually excised from the gel and digested with trypsin, as described previously (19). After being dehydrated with acetonitrile and dried in a SpeedVac centrifuge, the gels were re-swelled with 20-40 μl digestion solution containing 20 mM ammonium bicarbonate and 20 ng/μl of sequencing grade trypsin (Promega, Madison, WI, USA) and treated at 37°C overnight. The resultant peptides were extracted, desalted with ZipTip C_{18} columns (Millipore Corporation, Bedford, MA, USA) and eluted with 2.5 μl of 50% ACN containing 0.5% TFA. Peptide mass spectra were obtained by the ABI 4700 proteomics analyzer MALDI-TOF/TOF MS/MS (Applied Biosystems, Framingham, MA, USA), as described (20). Known contamination peaks such as keratin and autoproteolysis peaks were removed prior to the database search. Protein identification was performed using the MASCOT software (Matrix Science, London, UK) and all tandem mass spectra were searched against the NCBInr database, with a mass accuracy of within 200 ppm for the mass measurement, and within 0.5 Da for MS/MS tolerance window. Searches were performed without constraining protein molecular weight (Mr) or isoelectric point (pI) and species, and allowing for

Table I. Summary of identified proteins with MALDI-TOF/TOF tandem mass spectrometry.[a]

Spot no.	Protein ID	Swiss-Prot	Mr/pI	Score	MS/MS peptide/ matched peptide	Relative level (tumour/non-tumour)	Sequence coverage (%)
1	Heat shock protein 27 (HSP27)	P04792	22.4/7.83	358	5/13	2.23	52
2	Chloride intracellular channel 1 (CLIC1)	O00299	26.5/4.95	171	3/9	2.16	35
3	Glutathione S-transferase (GST)	P09211	23.6/5.43	344	3/14	3.22	57
4	Regucalcin (RGN)	Q15493	33.8/5.89	105	2/10	0.23	33
5	Inorganic pyrophosphatase (PPA)	Q15181	33.1/5.54	87	2/13	2.78	32
6	Ketohexokinase (KHK)	P50053	25.5/5.99	141	2/9	2.35	40
7	3-Hydroxyanthranilate 3,4-dioxygenase (HAAO)	P46952	32.7/5.72	83	2/9	2.51	32
8	Enoyl-CoA hydratase (ECH1)	Q13011	31.8/8.34	169	2/10	2.19	38
9	Nucleoside diphosphate kinase (NM23-H1)	P15531	19.8/5.42	396	6/16	2.08	51
10	Tubulin α-6 (TUBA6)	Q9BQE3	50.7/4.96	307	5/14	2.78	33
11	Tubulin ß-chain (TUBB)	P07437	50.3/4.78	118	3/13	2.15	27
12	Apolipoprotein A-1 (APOA1)	P02647	30.7/5.56	130	5/17	2.59	40
13	Proteasome activator subunit 1 isoform 2 (PA28α)	Q06323	28.7/6.28	104	3/9	0.45	17
14	DJ-1	Q99497	20/6.33	109	2/9	0.32	22
15	Triosephosphate isomerase (TPI1)	P60174	26.7/7.1	81	2/6	0.38	23

[a]The Mowse score of >75 was considered as significant ($p < 0.05$).

carbamidomethylation of cysteine and partial oxidation of methionine residues. Up to one missed tryptic cleavage was considered for all tryptic-mass searches. Protein scores >75 were considered to be significant ($p < 0.05$).

Immunoblot analysis. Twenty μg of total proteins from six pairs of HCC samples were separated by 12% SDS-PAGE and electro-transferred onto poly-vinylidene difluoride (PVDF) membranes by the SemiDry apparatus (Bio-Rad). The membranes, after blocking with 5% nonfat dry milk in TBS-T buffer (Tris-buffered saline, 0.1% Tween-20), were probed with one of the following antibodies: mouse monoclonal anti-human DJ-1 (Zymed® Laboratories, South San Francisco, CA, USA), rabbit polyclonal anti-human PA28α (Calbiochem®), and incubated at 4˚C overnight. ß-actin signal was detected by a

mouse monoclonal anti-human ß-actin antibody (Sigma-Aldrich, St. Louis, MO, USA) and used as an internal control. Goat anti-rabbit IgG horseradish peroxidase (ZyMED® Laboratories Inc, San Francisco, CA, USA) or goat anti-mouse IgG horseradish peroxidase (Upstate, Lake Placid, NY, USA) were used as secondary antibodies. Protein signals were detected using SuperSignal® West Pico chemiluminescent substrate (Pierce), and captured with the Multi Genius bio imaging system (Syngene, Frederick, MD, USA). Signal intensity was quantitatively analyzed using the GeneTools software (Syngene).

Immunohistochemistry. Immunohistochemical staining (IHC) of DJ-1 and PA28α in 15 pairs of paraffin-embedded, HBV-infected G1 tumour and non-tumour tissues were performed

using the Dako system as previously described (19,20). Briefly, sections of 4-μm thickness from both tumour and matched non-tumour tissue blocks were dewaxed, rehydrated and labelled for 60 min at room temperature with each of the two antibodies after conducting the antigen retrieval: anti-DJ-1 (1:20) and anti-PA28α (1:50), followed by detection with labelled dextran polymer conjugated with peroxidase and DAB$^+$-substrate chromagen solution. Slides were lightly counter-stained with hematoxylin before imaging. The staining levels were scored as negative, weak, moderate and strong based on the staining intensity by the pathologist. Negative and weak stainings were considered as negative whereas moderate and strong stainings were considered as positive.

Statistical analysis. Statistical differences in the levels of PA28α and DJ-1 in paired tumour and non-tumour tissues were analyzed by Fisher's exact test. $p < 0.05$ at two sides was considered as significant.

Results

Proteomic analysis of tumour and non-tumour tissues. To identify the potential tumour markers for early diagnostic purpose and elucidate the molecular changes at the early onset of heptocarcinogenesis, we compared the proteome profiles of three pairs of HBV-infected G1 tumour and adjacent non-tumour tissues. With the ImageMaster analysis software, more than 700 spots were detected in each gel, and in total, 35 spots were found to be consistently up- or down-regulated (>2.0-fold increase or decrease, Student t-test, $p < 0.05$) in at least two pairs of specimen. Fig. 1 shows the representative silver-stained 2-DE gel. After MALDI-TOF/TOF tandem mass spectrometry analysis and NCBInr database search
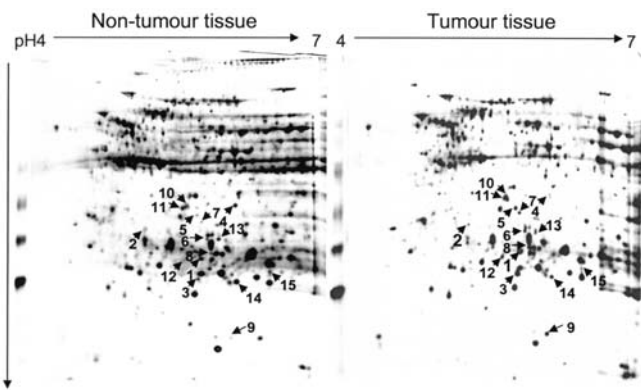

Figure 1. Differential proteome analysis of HBV-infected, well-differentiated HCC tumour and adjacent non-tumour tissues. Total protein lysates were separated by IEF using IPG DryStrip (180 mm, pH 4-7) and SDS-PAGE (12%). Silver-stained gels were scanned using the Personal SI densitometer (Molecular Dynamics) and analyzed using the ImageMaster 2D Elite software (GE Healthcare). The locations of identified proteins by MALDI-TOF/TOF tandem mass spectrometry are shown.

using Mascot software, 15 proteins were identified as listed in Table I. Their positions on the 2-DE map are annotated in Fig. 1. Of these identified proteins, 4 (RGN, DJ-1, PA28α and TPI) were down-regulated, whereas the other 11 were up-regulated, in the HBV-infected G1 tumours. Most of these identified proteins have been reported elsewhere (3,8,9,21), however, two proteins including PA28α (spot 13) and onco-protein DJ-1 (spot 14), that were not previously identified in the proteome analysis of HCC, were found to be down-regulated in the HBV-infected G1 tumours. Their representative 2-DE spot images with the MS/MS spectrum are shown in Fig. 2.
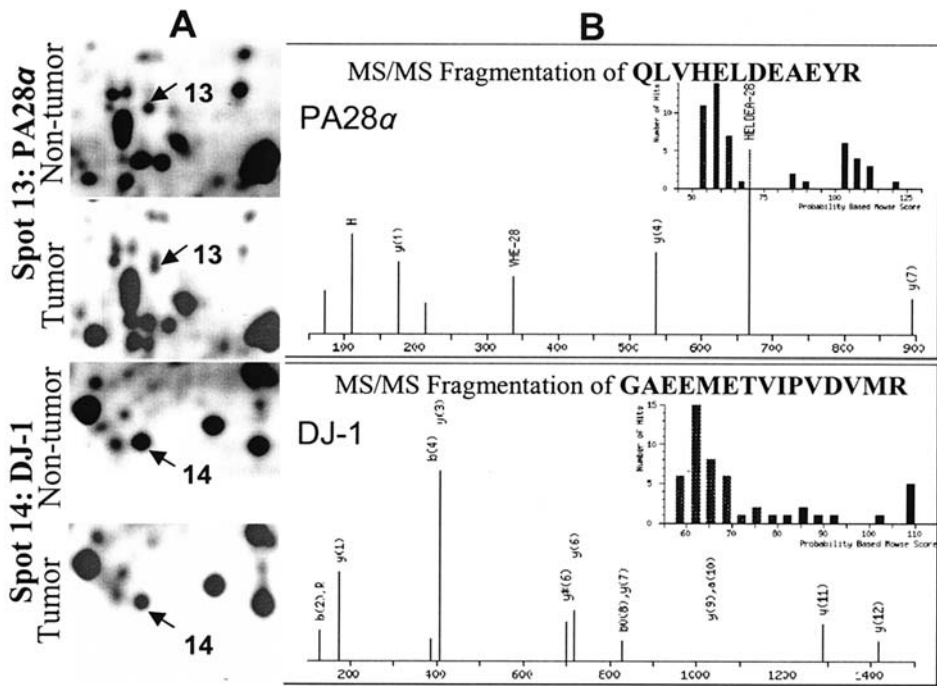

Figure 2. Identification of PA28α (spot 13) and DJ-1 (spot 14) by tandem mass spectrometry. (A) Zoom images from 2-DE gels showing spots containing PA28α and DJ-1. (B) MS/MS spectrum of the doubly charged precursor ion with *m/z* 1501.75 for peptide [199]QLVHELDEAEYR[210] of PA28α and the doubly charged precursor ion with *m/z* 1675.83 for peptide [13]GAEEMETVIPVDVMR[27] of DJ-1. Inserted figure is the Mowse score from database search.

Table II. Geneontology analysis of identified proteins.

Biological function	Protein	Subcellular localization	Locus
Anti-apoptosis	Heat shock protein 27	Cytoplasm	7q11.23
	Glutathione S-transferase	Cytoplasm	11q13.2
Ca^{2+} transport/signal transduction	Chloride intracellular channel 1	Nucleus	6p21.33
	Regucalcin	Cytoplasm	Xp11.3
Metabolism	Inorganic pyrophosphatase	Cytoplasm	10q22.1
	Ketohexokinase	Cytoplasm	2q23.3
	3-Hydroxyanthranilate 3,4-dioxygenase	Cytoplasm	2q21
	Enoyl-CoA hydratase	Mitochondria and peroxisome	19q13.1
	Triosephosphate isomerase	Cytoplasm	12p13.31
Metastasis	Nucleoside diphosphate kinase (NM23-H1)	Nuclear and cytoplasm	17q21.33
Structural molecules	Tubulin α-6	Cytoplasm	12q13.12
	Tubulin ß-chain	Cytoplasm	6p21.33
Transport	Apolipoprotein A-1	Secreted protein	11q23.3
Immune response	Proteasome activator subunit 1 isoform 2	Proteasome complex	14q11.2
Protein folding/Ras protein signal transduction	DJ-1	Nuclear and cytoplasm	1p36.23

Functional classification of the tumour marker molecules. To understand the biological relatives of the identified molecules with the onset of tumorigenesis in HBV-infected HCC, the identified 15 proteins were classified by their biological functions with the tools on www.geneontology.org (Table II). In brief, these proteins were functionally involved in enzyme activity (glyco-metabolism, lipid metabolism), immune activity, anti-apoptosis, Ca^{2+} binding/signal transduction, cell structure, protein folding and metastasis. Of the 15 proteins, eight were cytoplasmic, two were nucleic, one was mitochondrial, one was peroxisomal and one was secreted protein. Furthermore, by analyzing the chromosomal localization of these protein-encoding genes and genomic imbalance, we found a link. For example, the Hsp27 gene, located at 7q11.23, mapped within cancer-related chromosome region 7q11.23 (colon cancer and prostate cancer). On chromosome 1, chromosomal localization of oncogene DJ-1, 1p36.23, is associated with three cancer-related chromosome regions: 1p36 (ductal breast cancer), 1p36 (prostate cancer-brain cancer susceptibility) and 1p36.11 (liver cancer). Abnormality of these proteins may be involved in a network or oncogenic signal pathways required for the onset of the multi-step process in HCC development.

Immunoblotting and immunohistochemistry. As the reduced expression of the two proteins, PA28α and DJ-1, has not been identified previously, we further confirmed their differential expression by Western blotting in 6 pairs of HBV-infected G1 tumour and the adjacent non-tumour tissues. As shown in Fig. 3, expression levels of both PA28α and DJ-1 are shown in a case-dependent manner. However, the overall expression levels in the tumour tissues were lower than those in the matched non-tumour tissues. The levels of both DJ-1
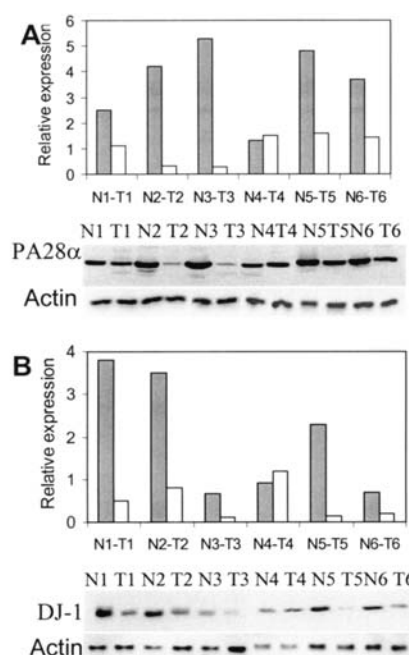

Figure 3. Western blotting of PA28α and DJ-1 in 6 pairs of HBV-infected, well-differentiated HCC tumour and adjacent non-tumour tissues. Proteins from each of the six pairs of tissue samples were separated by SDS-PAGE (12%) and transferred to PVDF membranes. Proteins were immunodetected using the respective primary antibodies and HRP-conjugated secondary antibody. Signals were captured with the Multi Genius bio imaging system and signal intensity was analyzed by the GeneTools software (Syngene). Average relative expression levels (±SD) in triplicate experiments were normalized to the level of ß-actin.

and PA28α were reduced by >3-fold (p<0.01) in tumours, compared to the non-tumour tissues.
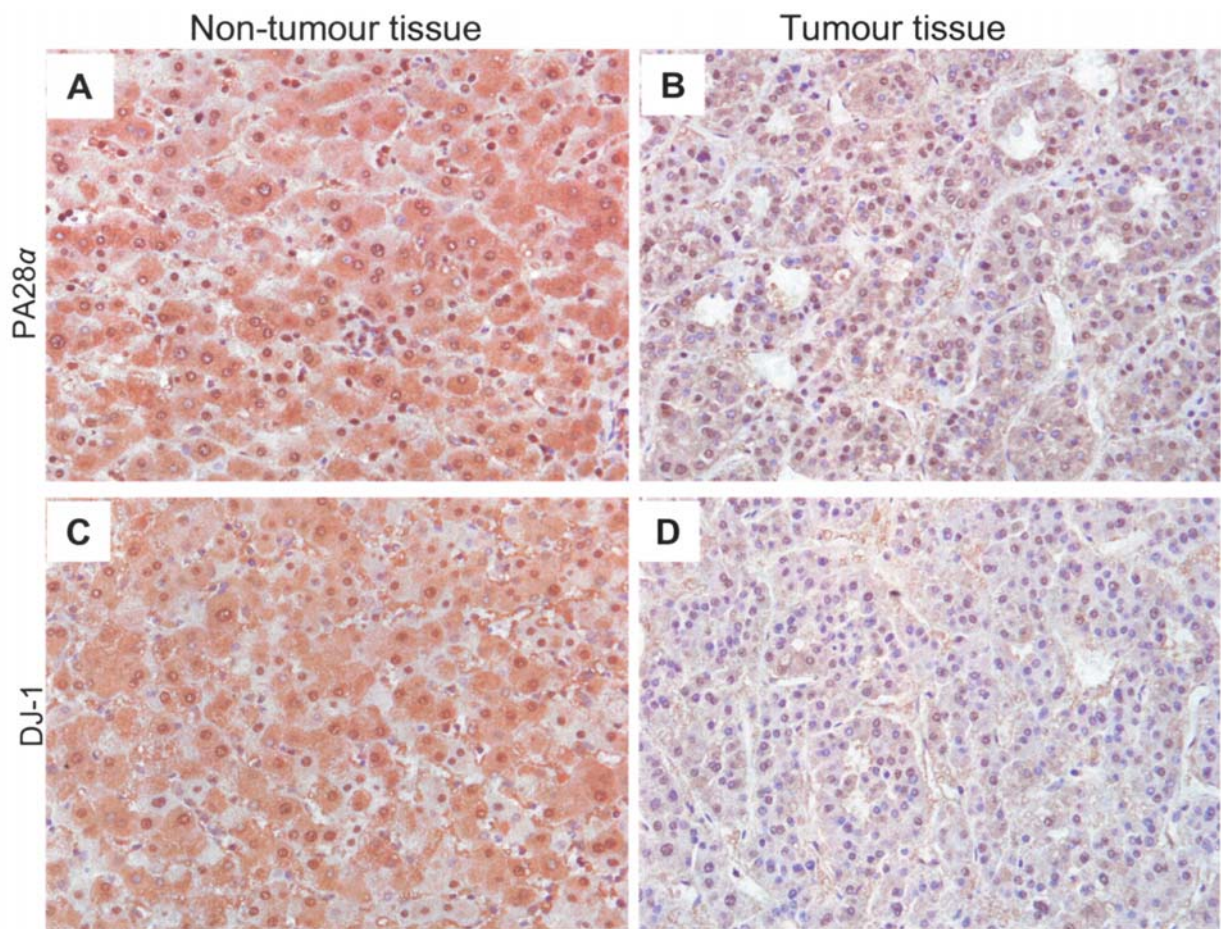
Figure 4. Representative immunostaining of PA28α and DJ-1 in HBV-infected, well-differentiated HCC tumour and adjacent non-tumour tissue sections. Paraffin-embedded sections were deparaffinized in xylene and rehydrated in graded alcohols. After unmasking antigen and removing endogenous peroxidases, sections were incubated for 1 h with antibody against PA28α and DJ-1 at room temperature, followed by detection with labelled dextran polymer conjugated with peroxidase and DAB⁺-substrate chromagen solution. Nuclei were lightly stained with Mayer's hematoxylin. The extent of staining was visually scored according to the staining intensity of cells. PA28α and DJ-1 were strongly stained in the non-tumour tissue cells (A and C), and weakly stained in tumour cells (B and D). Original magnification x400.

Table III. Summary of immunohistochemical staining of DJ-1 and PA28α in 15 pairs of paraffin-embedded, HBV-infected G1 hepatocellular carcinoma tissues.

Staining intensity[a]	Non-tumor tissues (n=15)	Tumor tissues (n=15)	Chi-square p-value[b]
DJ-1			
Negative	0	8	
Positive	15	7	0.002
PA28α			
Negative	0	6	
Positive	15	9	0.017

[a]Negative and weak staining were considered as negative; moderate and strong staining were considered as positive. [b]Fisher's exact test.

In situ expression of PA28α and DJ-1 was also examined in 15 paraffin-embedded HBV-infected G1 tumour and their adjacent non-tumour tissues. A representative immunostaining of DJ-1 and PA28α in paired tissues is shown in Fig. 4. As shown in Table III, all the 15 matched non-tumour tissues showed moderate to strong cytoplasmic staining of both DJ-1 and PA28α. However, PA28α was negatively stained in 6 of 15 tumour tissues (p=0.017), whereas DJ-1 was negatively stained in 8 of 15 tumour tissues (p=0.002). Therefore, DJ-1 and PA28α were down-regulated in most of the tested HBV-infected G1 tumours, compared to their adjacent non-tumour tissues.

Discussion

HCC is one of the most common cancers in the world and causes approximately one million deaths every year. Underlying the early molecular events of tumour onset may help to improve the diagnostic efficiency and develop more effective therapeutic strategies against HCC. With the aid of the proteomic approach integrated with a sophisticated bioinformatic tool and MALDI-TOF MS and MS/MS, we have identified 15 differentially expressed proteins from the HBV-infected G1 tumours. These proteins could be functionally interrelated and linked to the initiation of hepatocarcinogenesis. They were classified into several functional groups including

metabolism, signal transduction, apoptosis and metastasis (Table II). Although the majority of proteins identified in our study have been reported (4,8,9,21), several other proteins, e.g. DJ-1 and PA28α, have not previously been reported to be differentially expressed in HCC. In this study, we focused on these two proteins and their differential expression was further verified by immunoblotting and immunohistochemistry in a panel of HBV-infected G1 tumours. Although there is a need to further verify the reduced expression of PA28α and DJ-1 in more HBV-infected G1 tumours, and to investigate whether it is the same case in HCV-infected HCC tumours, the abnormal expression of these molecules and the involved biochemical pathways may elucidate, at least in part, the early events causing tumorigenesis in HBV-related HCC.

PA28α is an activator in the immunoproteasome system which has a pivotal role in the control of the immune response. PA28α enhances the generation of class I binding peptides by altering the cleavage pattern of the proteasome and is required for efficient antigen processing. Previous studies showed that PA28α responded to viral or bacterial infection and was up-regulated in the livers of lymphocytic choriomeningitis virus-infected mice (22), and its expression induced the production of HLA-class I in IFN-treated colon cancer cell line DLD-1 (23). The impaired expression of PA28α was also reported in cervical carcinoma lesions (24). However, HER-2/*neu* over-expression in fibroblasts reduced the level of MHC class I surface antigens by impairing the expression of PA28α and PA28ß and other proteasome components, thereby resulting in an immune escape phenotype of oncogene-transformed cells (25). Thus, a reduced level of PA28α may favour the tumour progression. In HCC, a lower level of PA28α, as demonstrated by immunoblotting and IHC (Figs. 2-4), in HBV-infected G1 may indicate an early decreased immune response to transformation and onset of tumour formation. Clinically, we proposed that the level of PA28α could be used as an immunological indicator, together with histological analysis, to assess the hepatocarcinogenesis.

DJ-1 is an integral mitochondrial protein that may have important functions in regulating mitochondrial physiology. It interacts, as an oncoprotein, with Daxx and inhibits apop-tosis signal-regulating kinase 1 activity and cell death (26). Several lines of evidence suggested that DJ-1 played a role in tumorigenesis in breast cancer, non-small cell lung carcinoma and prostate cancer (27-29). Moreover, DJ-1 positively regulates p53 through Topors-mediated sumoylation (30), and is recognized as a key negative regulator of PTEN that may be a useful prognostic marker for cancer (31). Sumoylation on a lysine residue at K130 and K130 mutation abrogated all of the functions of DJ-1, including *ras*-dependent transform-ation, cell growth promotion and anti-UV-induced apoptosis activities (32). Currently, Pardo *et al* found that DJ-1 was highly expressed and secreted in the malignant melanoma cells and considered as a potential serum biomarker in patients (33). In patients with breast cancer, DJ-1 was detected in the serum of 37% as a circulating tumour antigen (27). From our study, we observed the down-regulation of DJ-1 in the early stage of HBV-infected HCC (Figs. 2-4). The reduced level of DJ-1 may indicate the abnormal pathophysiological state of mitochondria and mitochondrial disease initiates the tumori-genesis in HBV-infected HCC. As it has been described as a

circulating tumour antigen in serum from 37% of patients with breast cancer (27), we will study whether this is the case in HBV-infected HCC to further assess its clinical value as an early diagnostic biomarker in patients.

In summary, we present here the comparative analysis of proteome profiles from HBV-infected G1 tumour and adjacent non-tumour tissues, and identify the differentially expressed molecules which are potentially responsible for the early onset of tumorigenesis and are valuable markers for early diagnosis in patients with HCC. We show the involvement of molecules in a variety of pathways, including signal transduction, metabolism and anti-apoptosis in the early stage of HCC. Although we have only validated our results in a limited number of clinical specimens, the reduced expression of the molecules, PA28α and DJ-1, could be a promising novel biomarker for malignancy detection and diagnosis in HBV-infected HCC.

Acknowledgements

References

1. Chen CJ and Chen DS: Interaction of hepatitis B virus, chemical carcinogen, and genetic susceptibility: multistage hepatocarcino-genesis with multifactorial etiology. Hepatol 36: 1046-1049, 2002.
2. Fujiyama S, Tanaka M, Maeda S, Ashihara H, Hirata R and Tomita K: Tumor markers in early diagnosis, follow-up and management of patients with hepatocellular carcinoma. Oncology 62: 57-63, 2002.
3. Li C, Hong Y, Tan YX, *et al*: Accurate qualitative and quantitative proteomic analysis of clinical hepatocellular carcinoma using laser capture microdissection coupled with isotope-coded affinity tag and two-dimensional liquid chromatography mass spectrometry. Mol Cell Proteomics 3: 399-409, 2004.
4. Lee IN, Chen CH, Sheu JC, *et al*: Identification of human hepatocellular carcinoma-related biomarkers by two-dimensional difference gel electrophoresis and mass spectrometry. J Proteome Res 4: 2062-2069, 2005.
5. Luk JM, Lam CT, Siu AF, *et al*: Proteomic profiling of hepato-cellular carcinoma in Chinese cohort reveals heat-shock proteins (Hsp27, Hsp70, GRP78) up-regulation and their associated prognostic values. Proteomics 6: 1049-1057, 2006.
6. Zeindl-Eberhart E, Haraida S, Liebmann S, *et al*: Detection and identification of tumor-associated protein variants in human hepatocellular carcinomas. Hepatol 39: 540-549, 2004.
7. Yokoyama Y, Kuramitsu Y, Takashima M, *et al*: Proteomic profiling of proteins decreased in hepatocellular carcinoma from patients infected with hepatitis C virus. Proteomics 4: 2111-2116, 2004.
8. Kim W, Lim S, Kim JS, *et al*: Comparison of proteome between hepatitis B virus- and hepatitis C virus-associated hepatocellular carcinoma. Clin Cancer Res 9: 5493-5500, 2003.
9. Liang CR, Leow CK, Neo JC, *et al*: Proteome analysis of human hepatocellular carcinoma tissues by two-dimensional differ-ence gel electrophoresis and mass spectrometry. Proteomics 5: 2258-2271, 2005.
10. Park KS, Cho SY, Kim H and Paik YK: Proteomic alterations of the variants of human aldehyde dehydrogenase isozymes correlate with hepatocellular carcinoma. Int J Cancer 97: 261-265, 2002.
11. Feng JT, Liu YK, Song HY, *et al*: Heat-shock protein 27: a potential biomarker for hepatocellular carcinoma identified by serum proteome analysis. Proteomics 5: 4581-4588, 2005.
12. Takashima M, Kuramitsu Y, Yokoyama Y, *et al*: Overexpression of alpha enolase in hepatitis C virus-related hepatocellular carcinoma: association with tumor progression as determined by proteomic analysis. Proteomics 5: 1686-1692, 2005.

13. Lee IN, Chen CH, Sheu JC, *et al*: Identification of complement C3a as a candidate biomarker in human chronic hepatitis C and HCV-related hepatocellular carcinoma using a proteomics approach. Proteomics 6: 2865-2873, 2006.
14. Ding SJ, Li Y, Tan YX, *et al*: From proteomic analysis to clinical significance: overexpression of cytokeratin 19 correlates with hepatocellular carcinoma metastasis. Mol Cell Proteomics 3: 73-81, 2004.
15. Kuramitsu Y, Harada T, Takashima M, *et al*: Increased expression and phosphorylation of liver glutamine synthetase in well-differentiated hepatocellular carcinoma tissues from patients infected with hepatitis C virus. Electrophoresis 27: 1651-1658, 2006.
16. Nissom PM, Lo SL, Lo JC, *et al*: Hcc-2, a novel mammalian ER thioredoxin that is differentially expressed in hepatocellular carcinoma. FEBS Lett 580: 2216-2226, 2006.
17. Iizuka N, Oka M, Yamada-Okabe H, *et al*: Comparison of gene expression profiles between hepatitis B virus- and hepatitis C virus-infected hepatocellular carcinoma by oligonucleotide microarray data on the basis of a supervised learning method. Cancer Res 62: 3939-3944, 2002.
18. Desmet VJ, Gerber M, Hoofnagle JH, Manns M and Scheuer PJ: Classification of chronic hepatitis: diagnosis, grading and staging. Hepatol 19: 1513-1520, 1994.
19. Zhang D, Tai LK, Wong LL, Sethi SK and Koay ES: Proteomics of breast cancer: enhanced expression of cytokeratin 19 in human epidermal growth factor receptor type 2 positive breast tumors. Proteomics 5: 1797-1805, 2005.
20. Zhang D, Tai LK, Wong LL, Chiu LL, Sethi SK and Koay ESC: Proteomic study reveals that proteins involved in metabolic and detoxification pathways are highly expressed in HER-2/*neu*-positive breast cancer. Mol Cell Proteomics 4: 1686-1696, 2005.
21. Li C, Tan YX, Zhou H, *et al*: Proteomic analysis of hepatitis B virus-associated hepatocellular carcinoma: Identification of potential tumor markers. Proteomics 5: 1125-1139, 2005.
22. Khan S, van den Broek M, Schwarz K, de Giuli R, Diener PA and Groettrup M: Immunoproteasomes largely replace constitutive proteasomes during an antiviral and antibacterial immune response in the liver. J Immunol 167: 6859-6868, 2001.
23. Miyagi T, Tatsumi T, Takehara T, Kanto T, Kuzushita N, Sugimoto Y, *et al*: Impaired expression of proteasome subunits and human leukocyte antigens class I in human colon cancer cells. J Gastroenterol Hepatol 18: 32-40, 2003.
24. Ritz U, Momburg F, Pilch H, Huber C, Maeurer MJ and Seliger B: Deficient expression of components of the MHC class I antigen processing machinery in human cervical carcinoma. Int J Oncol 19: 1211-1220, 2001.
25. Herrmann F, Lehr HA, Drexler I, *et al*: HER-2/*neu*-mediated regulation of components of the MHC class I antigen-processing pathway. Cancer Res 64: 215-220, 2004.
26. Junn E, Taniguchi H, Jeong BS, Zhao X, Ichijo H and Mouradian MM: Interaction of DJ-1 with Daxx inhibits apoptosis signal-regulating kinase 1 activity and cell death. Proc Natl Acad Sci USA 102: 9691-9696, 2005.
27. Le Naour F, Misek DE, Krause MC, *et al*: Proteomics-based identification of RS/DJ-1 as a novel circulating tumor antigen in breast cancer. Clin Cancer Res 7: 3328-3335, 2001.
28. MacKeigan JP, Clements CM, Lich JD, Pope RM, Hod Y and Ting JP: Proteomic profiling drug-induced apoptosis in non-small cell lung carcinoma: identification of RS/DJ-1 and RhoGDIalpha. Cancer Res 63: 6928-6934, 2003.
29. Hod Y: Differential control of apoptosis by DJ-1 in prostate benign and cancer cells. J Cell Biochem 92: 1221-1233, 2004.
30. Shinbo Y, Taira T, Niki T, Iguchi-Ariga SM and Ariga H: DJ-1 restores p53 transcription activity inhibited by Topors/p53BP3. Int J Oncol 26: 641-648, 2005.
31. Kim RH, Peters M, Jang Y, *et al*: DJ-1, a novel regulator of the tumor suppressor PTEN. Cancer Cell 7: 263-273, 2005.
32. Shinbo Y, Niki T, Taira T, *et al*: Proper SUMO-1 conjugation is essential to DJ-1 to exert its full activities. Cell Death Differ 13: 96-108, 2006.
33. Pardo M, Garcia A, Thomas B, *et al*: The characterization of the invasion phenotype of uveal melanoma tumour cells shows the presence of MUC18 and HMG-1 metastasis markers and leads to the identification of DJ-1 as a potential serum biomarker. Int J Cancer 119: 1014-1022, 2006.